The Journal of Engineering and Exact Sciences – JCEC, Vol. 05 N. 01 (2019)
journal homepage: https://periodicos.ufv.br/ojs/jcec
doi: https: 10.18540/jcecvl5iss1pp0090-0099
OPEN ACCESS – ISSN: 2527-1075

AN INSILCO STUDY OF 1,1-DIFLUORO-2-METHOXYPROPANE REACTION MECHANISM WITH THE BROMINE MONOXIDE (BrO) RADICAL

M. A. RUFAI [1, *], U. ADAMU[1], S. GIDEON[1] and S. UBA[1]
[1]Ahmadu Bello University, Department of Chemistry, Zaria, Kaduna State, Nigeria
*Corresponding author. Ahmadu Bello University, Department of Chemistry, Zaria, Kaduna State, Nigeria, Phone: +2347033748067
e-mail addressl: marufai2424@gmail.com (M. A. Rufai).

ARTICLE INFO
Article history:
Received 2018-06-05
Accepted 2018-08-27
Available online 2019-03-08

palabras clave
1,1-difluoro-2-metoxipropano
DFT
CFCs
BrO)

keywords
1,1-difluoro-2-methoxypropane
DFT
CFCs
BrO

ABSTRACT

An Insilco study was carried out on the thermochemistry, mechanism and kinetics of the Hydrogen abstraction reaction of 1,1-difluoro-2-methoxypropane ($CH_3CH(OCH_3)CHF_2$) with the bromine monoxide radical (BrO) using the Density Functional Theory (DFT) based M06-2X/6311++G** method. The energy values were immediately improved via optimization at DFT/M06-2X/6-311++G(2df,2p) level (single-point calculations) of the reacting species involved. The Monte Carlo search on the investigating hydrofluoroether (HFE) showed nine conformers with the lowest global minimum conformer being predicted and considered for this work. The results of this study showed that the atmospheric oxidation reaction of $CH_3CH(OCH_3)CHF_2$ with the BrO radical proceeded in four (4) plausible reaction routes. The total experimental rate of $4.34*10^{-06}$ cm^{-3} $molecule^{-1}$ sec^{-1} for HFE + BrO reaction was estimated with atmospheric lifetime (ALT)/global warming potential (GWP) of 1.80 years and 165.30 respectively. The 3D potential energy surfaces (PES) for the reaction was however constructed at absolute temperature of 298.15 K.

RESUMEN

*Se realizó un estudio de Insilco sobre la termoquímica, el mecanismo y la cinética de la reacción de abstracción de hidrógeno de 1,1-difluoro-2-metoxipropano ($CH_3CH(OCH_3)$ CHF_2) con el radical de monóxido de bromo (BrO) utilizando la teoría de la función de densidad (DFT) basado en el método M06-2X / 6-311 ++ G **. Los valores de energía se mejoraron inmediatamente a través de la optimización a nivel de DFT / M06-2X / 6-311 ++ G (2df, 2p) (cálculos de punto único) de las especies reactivas implicadas. La búsqueda de Monte Carlo en el hidrofluoroéter investigador (HFE) mostró nueve confórmeros con el confórmero mínimo global más bajo que se predijo y se consideró para este trabajo. Los resultados de este estudio mostraron que la reacción de oxidación atmosférica de CH_3CH $(OCH_3)CHF_2$ con el radical BrO procedió en cuatro (4) rutas de reacción plausibles. La tasa experimental total de 4.34 * 10-06 cm^{-3} molécula-1 seg-1 para la reacción HFE + BrO se estimó con la vida atmosférica (ALT) / potencial de calentamiento global (GWP) de 1.80 años y 165.30, respectivamente. Sin embargo, las superficies de energía potencial 3D (PES) para la reacción se construyeron a una temperatura absoluta de 298,15 K.*

NOMENCLATURE

ALT: Atmospheric lifetime

BrO: Bromine monoxide radical

CFCs: Chlorofluorocarbons

DFT: Density functional theory

GWP: Global warming potential

HFEs: Hydrofluoroethers

IRC: Intrinsic reaction coordinate

PC: Product complex

PES: Potential Energy Surface

RC: Reactant complex

TS: Transition state

1. INTRODUCTION

The less reactivity and easy liquefaction are two main chemical properties that qualify Chlorofluorocarbons (CFCs) as good raw materials in the production of foam blowing agents, electronic detergents, aerosols, deodorant sprays, refrigerators, paint sprays, cleaning agents, furniture polishes, propellants, semiconductors etc. (Deka and Mishra, 2014; Guo *et al.*, 2018; Philip, 1996). Researchers have shown that CFCs derivatives pose environmental hazards to ozone by diffusing into stratosphere and deplete it at a rate faster than it can be replaced in the atmosphere (Baidya *et al.*, 2017; Garfield, 1988; Molina and Rowland, 1974; Orkin *et al.*, 1999; Papadimitriou *et al.*, 2007; Rowland, 1996; Rohrer and Berresheim, 2006; Rowley and Ferracci, 2014; WMO, 2010). For this fact, international restrictions and warning were placed on usage of CFCs as agreed upon in the Montreal Protocol (Good *et al.*, 1998; Ye *at al.*, 2016). Instead, alternative compounds with less or no posing ability to ozone is recommended as substantial substitutes for the CFCs (Espinosa-Garcia, 2003; Galano *et al.*, 2010; MWO, 2010). Hydrofluoroethers (HFEs) and hydrofluoroalcohols (HFAs) (Mabury *et al.*, 2006; White and Martell, 2015), have been discovered as substantial substitutes for CFCs with numerous applications ranging from refrigeration, cleaning, foam blowing, propelling, painting, solvents, pesticides, varnishes in laboratories etc. (Deka and Mishra, 2014; Hashemi and Saheb, 2017; Hurley *et al.*, 2004; Laszlo *et al.*, 1997; Prather and Spivakovsky, 1990; Sako *et al.*, 1996; Wang *et al.*, 2009). The presence of $-\mathrm{O}-$ linkage between these series increases their chemical reactivity in the atmosphere which accounts for the chemistry of their short lifetime and lesser atmospheric effects compare to CFCs (Baidya *et al.*, 2017; Gour *et al.*, 2016).

The study of $CH_3CH(OCH_3)CHF_2$ with BrO radicals is an important atmospheric oxidation reaction that will provide information on the tropospheric reactivity of HFEs and also help to find degradation pathways of HFEs in the atmosphere. Hence, it is very necessary/vital to dig into the atmospheric chemistry of the HFEs for their better understanding as substantial substitutes for CFCs and to determine more of their impacts on the environment.

Many experimental studies carried out on the related study of this kind only provided the overall rate constants but found it very difficult to reveal the actual mechanism and the true reaction picture especially when the reaction is multi channels. However, with computational study the detailed mechanism, thermochemistry of multi channels of reactions, the tunneling correction and overall rate constant can be estimated accurately and simultaneously. This as a modern computational chemistry technique is very simple, time and cost saver, accurate and very fast compares to wet laboratory method.

The main objective of this study was to make an Insilco study on reaction of $CH_3CH(OCH_3)CHF_2$ with BrO radical using computational techniques. And also aimed at studying the computational kinetics of H-abstraction reaction of $CH_3CH(OCH_3)CHF_2$ by BrO radical which involves four (4) H-abstraction positions of $-\mathrm{CHF_2}, -\mathrm{OCH_3}, -\mathrm{CH}$ and $-\mathrm{CH_3}$ as shown in the chemical reactions R1-R4.

$$CH_3CH(OCH_3)CHF_2 + BrO \rightarrow CH_3CH(OCH_3)CF_2 + HOBr \quad (R1)$$

$$CH_3CH(OCH_3)CHF_2 + BrO \rightarrow CH_3C(OCH_3)CHF_2 + HOBr \quad (R2)$$

$$CH_3CH(OCH_3)CHF_2 + BrO \rightarrow CH_3CH(OCH_2)CHF_2 + HOBr \quad (R3)$$

$$CH_3CH(OCH_3)CHF_2 + BrO \rightarrow CH_2CH(OCH_3)CHF_2 + HOBr \quad (R4)$$

The study by Christensen *et al.*, 1998 on HFE – 7200 ($C_4F_9OC_2H_5$) with OH radicals at 295 K revealed that HFE – 7200 has k (OH + n- $C_4F_9OC_2H_5$) = (6.4 ± 0.7) * 10^{-14} $cm^{-3}molecule^{-1}$ s^{-1}, k (OH + i- $C_4F_9OC_2H_5$) = (7.7 ± 0.8) * 10^{-14} $cm^{-3}molecule^{-1}$ s^{-1} and atmospheric lifetime of 0.9 and 0.7 years respectively. Also, computational study of H-abstraction reactions from $CH_3OCH_2CH_2Cl$/ $CH_3CH_2OCH_2CH_2Cl$ by Cl atom and OH radical showed that their atmospheric lifetime are 39 hrs. and 19 hrs. respectively. (Gour *et al.*, 2016). Thus, the presence of an atom of Br, Cl, I etc. in an atmosphere is a chemical set back to ozone layer (Deka and Mishra, 2014; Laszlo *et al.*, 1997; Wofsy *et al.*, 1975; Yang *et al.*, 2007).

To ascertain fluorinated ethers as substantial alternatives for CFCs, there is necessity for proper and several Insilco/wet laboratory studies on them so as to determine them as substantial candidates capable of replacing CFCs.

2. MATERIALS AND METHODS

2.1 Samples used (HFEs and radical)

1,1-difluoro-2-methoxypropane (HFE), BrO radical were used for this Insilco study (Anderson, 1987; Baidya *et al.*, 2017; Hashemi & Saheb, 2017; Schlager *et al.*, 2012; MWO, 2010). The 3D structures of HFEs/radical were drawn using Spartan 14 v 112 suite licensed software (Spartan '14, 2013).

2.2 Computational Procedures

The Spartan 14 v 112 suite licensed software was used for all the electronic calculations. The geometry optimization of all chemical species involved in the reaction were carried out using density functional theory (DFT) based M06-2X method with the 6-311++G** basis set (Spartan '14, 2013). To improve the energy values, 6-311++G(2df,2p) single-point calculations were immediately performed using same DFT method. Earlier related studies on computational kinetics proved that, theoretical thermochemistry and kinetics of reaction can be modeled accurately and provides reliable results when the DFT with M06-2X level of theory is employed (Baidya *et al.*, 2017; De Carvalho and Roberto-Neto, 2018; Hashemi and Saheb, 2017; White and Martell, 2015).

The minimum energy equilibrium structure obtained at each stationary point has all real frequencies meanwhile transition state possesses one imaginary frequency. The imaginary frequency in transition state corresponds to the coupling of stretching modes of the breaking C–H. Transformation from the reactant to product via the transition state (TS) along the minimum energy path was confirmed with the help of intrinsic reaction coordinate (IRC) calculations at the M06-2X level of DF theory (Baidya *et al.*, 2017; Gour *et al.*, 2016). IRC calculations confirmed the formation of pre and post-reaction complexes of the reactant/product molecule with the BrO radical or HOBr in both the entry and exit of each reaction channel.

The rate constants (k) for H–abstraction reactions were obtained from the reaction basic steps involved according to equation 5-6.

$$HFEs + BrO \rightleftharpoons TS1 \tag{5}$$

$$TS1 \rightarrow P + HOBr \tag{6}$$

The rate coefficients (k), change in enthalpy ($\Delta_{\mathbf{r}}H^{o}{}_{rxn}$), change in free Gibb's energy ($\Delta_{\mathbf{r}}G^{o}{}_{rxn}$) and change in energy ($\Delta_{\mathbf{r}}E^{o}{}_{rxn}$) of each radical's reaction channels were computed according to the view of Roussel, 2009; Siaka and his coworkers in 2017; Truhlar and his coworkers in 1996 as in equation 7-10.

$$k = \sigma_r \Gamma \frac{k_B T}{h} \frac{Q_{TS}{}^{\dagger}}{Q_R} e^{-\frac{\Delta E^{\neq}}{RT}} \tag{7}$$

$$\Delta_{\mathbf{r}} H^{o}{}_{rxn} = \sum\nolimits_{prod.} \Delta_f H_{prod.} - \sum\nolimits_{react.} \Delta_f H_{react.} \tag{8}$$

$$\Delta_r G^{o}{}_{rxn} = \Delta_{\mathbf{r}} H^{o}{}_{rxn} - T\Delta_r S^{o}{}_{rxn} \tag{9}$$

$$\Delta_r E^{o}{}_{rxn} = \sum\nolimits_{prod.} \Delta_f E_{prod.} - \sum\nolimits_{react.} \Delta_f E_{react.} \tag{10}$$

The change in enthalpy as well as Gibb's free energy of each transition states were estimated using expressions 11-12

$$\Delta \mathrm{H}^{\#} = \sum\nolimits_{\mathrm{prod.}} \Delta_{\mathbf{f}} \mathrm{H}^{\#} - \sum\nolimits_{\mathrm{react.}} \Delta_{\mathrm{f}} \mathrm{H}_{\mathrm{react.}} \tag{11}$$

$$\Delta \mathrm{G}^{\#} = \Delta \mathrm{H}^{\#} - T\Delta S^{\#} \tag{12}$$

The total rate coefficient was calculated using equation 13

$$\mathrm{k} = \mathrm{k}_{\mathrm{R}_1} + \mathrm{k}_{\mathrm{R}_2} + \mathrm{k}_{\mathrm{R}_3} + \mathrm{k}_{\mathrm{R}_4} \tag{13}$$

The branching ratios (BR) for the Hydrogen abstraction reaction channels of each radical, which is reported by Deka and Mishra, 2014 to have been represented the individual contribution of a reaction channel toward overall reaction rate were computed using an expression 14.

$$Branching\ ratio = \frac{k}{k_{Total}} * 100 \tag{14}$$

The E_a values of all reaction channels for each radical were determined using expression 15.

$$E_a = \Delta G^{\dagger} = \Delta G^{\#} - \sum \Delta G_r \tag{15}$$

The atmospheric lifetime of HFE + BrO radical was computed using an expression 16

$$\tau_{eff} = \tau_{BrO} \tag{16}$$

The 100-time horizon Global warming potential (GWP) of HFE is estimated in accordance to the view of Baidya and his colleagues in 2017 as expressed in equation 17

$$GWP_i(H) = \frac{\int_O^H RF_i\,(t)dt}{\int_O^H RF_{CO_2}\,(t)dt} = \frac{AGWP_i(H)}{AGWP_{CO_2}(H)} \tag{17}$$

3. RESULTS AND DISCUSSION

3.1 Sample conformers

Fig. **1** shows the nine possible conformers of 1,1-difluoro-2-methoxypropane molecule ranging from the lowest to highest energy conformers.

Monte Carlo's search was (conformational analysis) performed on $H_3CCH(OCH_3)CHF_2$ molecule by selecting Set up/Calculation/Conformational search under the application menu. MMFF force field was selected with maximum iteration number entered under the Mini tab. The default (1000) for maximum number was activated from the conformational search tab. The operation was then started with file name given. The result of this operational search showed nine conformers as illustrated in **Fig. 1.** From the analysis, conformer **A** (0.10 kcal mol^{-1}) had the lowest global minimum predicted. This search was aimed at identifying the possible conformers of $H_3CCH(OCH_3)CHF_2$ molecule with their respective global minima and to select the most stable conformer. Conformers with higher global minima were not considered since they are unstable (Baidya *et al.*, 2017). The generated conformers were arranged in **Fig. 1** in order of increasing in their energy stabilities. So, with reference to **Fig. 1**, conformer **I** (2.88 kcal mol^{-1}) has the highest energy predicted and thus the most unstable.

Fig. **2** shows the 3D structures of the optimized reacting species while **Fig**. **3** depicts 3D PES of H-atom abstraction from HFE with the radical.

Table 1 and **3** show the results of calculated energies and enthalpies (in kJ mol^{-1}) of the reacting species with BrO radical at DFT/M06-2X/6-311++G** level while the **Table 2** and **4** show the results on single-point calculation which was aimed at improving the reacting species energies as well as their enthalpies (in kJ mol^{-1}) at DFT/M06-2X/6-311++G(2df,2p) level.

Table 5 shows the thermodynamics calculation results of H-abstraction reaction routes that were performed at DFT/M06-2X/6-311++G** level with BrO radical. These results show that reaction through the routes R1 and R2 were exothermic in nature i.e. $\Delta_r H^{o}{}_{rxn} < 0$ and thermodynamically favorable while R3 and R4 routes followed endothermic reactions ($\Delta_r H^{o}{}_{rxn} > 0$), thus the routes (R2 and R3) were thermodynamically unfavored. The $\Delta_r E^{o}{}_{rxn}$ across the four routes of this reaction proved that R2 and R4 routes have high possibility of H-abstraction than R1 and R3 since they (R2 and R4) had lower $\Delta_r E^{o}{}_{rxn}$. Also, the negative values of $\Delta_r G^{o}{}_{rxn}$ across all the reaction routes indicated that the obtained products were thermodynamically feasible. Hence, R2 is more feasible. However, an improved and further thermodynamics single-point calculation (DFT/M06-2X/6-311++G(2df,2p)) results in **Table 6** illustrates the endothermic nature of reaction via R1 and R4 but exothermic along R2 and R3 respectively. Also, $\Delta_r G^{o}{}_{rxn}$ across reaction routes revealed that, the product obtained were thermodynamically feasible (R2 also more feasible).

Tables **7** and **8** reveal that reaction of BrO radical with the sample proceeded in two steps: (1) transition state formation and (2) product formation. According to the Gibb's free energies of the two steps computed, the rate determining step (RDS) of each reaction channel was identified on the basis of $\Delta G_1 > \Delta G^{\#}$. Thus, the second steps i.e. product formation were the RDS. The rate determining steps are the slowest steps in the reaction between the HFE and the radical specie that was investigated.

The results from Tables **9** and **10** show that there were four H-atom abstraction carbon sites of $H_3CCH(OCH_3)CHF_2$ which are $-CHF_2$, $-CH$, $-OCH_3$ and $-CH_3$ groups. This eventually led to formation of four transition states (TS1, TS2, TS3 and TS4) as the sample was reacting with BrO radical. For each transition state of the radical investigated with sample, the C–H bond of the abstracting hydrogen atom and newly formed bond between H and O atoms were noted. The intrinsic reaction coordinates (IRC) calculation performed on all transition states at the same level were characterized by the occurrence of an imaginary frequencies as illustrated in same Tables (**9** and **10** respectively). This therefore proved that there exists chemical connection between transition states and reactants as well as products of all reaction channels for radical involved. Also, during entrance and exit channels (R1–R4) of this reaction, pre–reactive complexes (RC1, RC2, RC3 and RC4) and post–reactive complexes (PC1, PC2, PC3 and PC4) formed have been validated as recommended by Baidya and his coworkers in 2017. In addition, formation of hydrogen bond was observed in the pre–reactive and post–reactive complexes between Oxygen atom of BrO radical with H-atom in the $H_3CCH(OCH_3)CHF_2$ which was as a result of weak force of attraction. Thus, this implies that all the reaction channels can even proceed in an indirect mechanism manner.

Table **11** illustrates the variations in BR_{BrO}, k_{BrO}, as well as Ea_{BrO} of sample's reaction with BrO radical investigated. The k_{BrO} along the channels R1 and R2 were greater than the k_{BrO} across channels R3 as well as R4. The extremely higher BR_{BrO} value along channel R1 is due to the chemical influence of Fluorine atoms at C1.

3.2 Rate constant computation

The rate constants for reaction channels R1, R2, R3 and R4 were computed using the TST equation (7) couple with Wigner's H-abstraction tunneling correction at an absolute temperature of 298.15 K. The lowest energy conformer of $H_3CCH(OCH_3)CHF_2$ molecule was considered for H-abstraction reaction with atmospheric radical (BrO). The sample's reaction with radical passed through four channels with transition states: TS1, TS2, TS3 and TS4 respectively been formed. The total rate constant value at 298.15 K was estimated according to an expression (13). The computed rate constant values obtained using an improved single-point calculation (DFT/M06-2X/6-311++G(2df,2p) were given in **Table** 11. The total estimated rate for HFE + BrO was $4.34*10^{-06}$ cm^{-3} $molecule^{-1}$ sec^{-1}.

3.3 Atmospheric implications

The atmospheric lifetime of $H_3CCH(OCH_3)CHF_2$ (τ_{eff}) was estimated via the assumption that its atmospheric removal is through its reaction with BrO radical. So, it was estimated using expression (16). i.e.

$$\tau_{eff} = \tau_{BrO} \qquad (16)$$

Where, $\tau_{BrO} = (k_{BrO} * [BrO])^{-1}$ (18)

If the global average atmospheric BrO radical concentration is taken as $3.0*10^{7}$ molecule cm^{-3} and the calculated total value of k_{BrO} is $4.34*10^{-06}$ cm^{-3} $molecule^{-1}$ sec^{-1}. The atmospheric lifetime of $H_3CCH(OCH_3)CHF_2$ have been recorded as 1.8 years.

3.4 Global warming potentials (GWPs)

The global warming potentials of $H_3CCH(OCH_3)CHF_2$ molecule was estimated at the DFT/M06-2X/6-311++G(2df,2p) based on the integrated-time radiative forcing spontaneous radiation of 1 kg CO_2 as a reference gas (Baidya *et al.*, 2017; Orkin *et al.*, 1999). The HFE's GWPs was found relative to the CO_2 reference information using an equation 17. The GWPs obtained for HFE in 100-year time horizon is 165.30 while the GWP for CFC-11, the most vital CFC with numerous applications (100-year time horizon) is reported as 4600 (Baidya *et al.*, 2017). In comparison, $H_3CCH(OCH_3)CHF_2$ with shorter estimated atmospheric lifetime and lower GWP is of lesser atmospheric and environmental effects than CFCs.

4. FIGURES

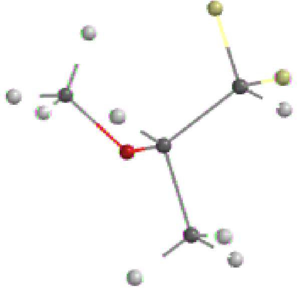

A

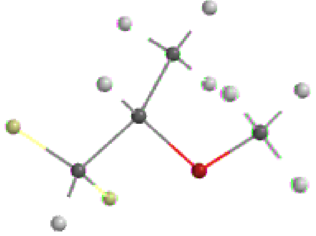

B

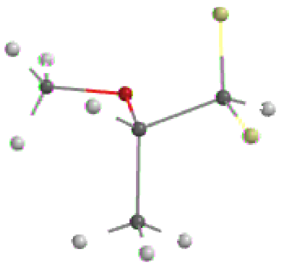

C

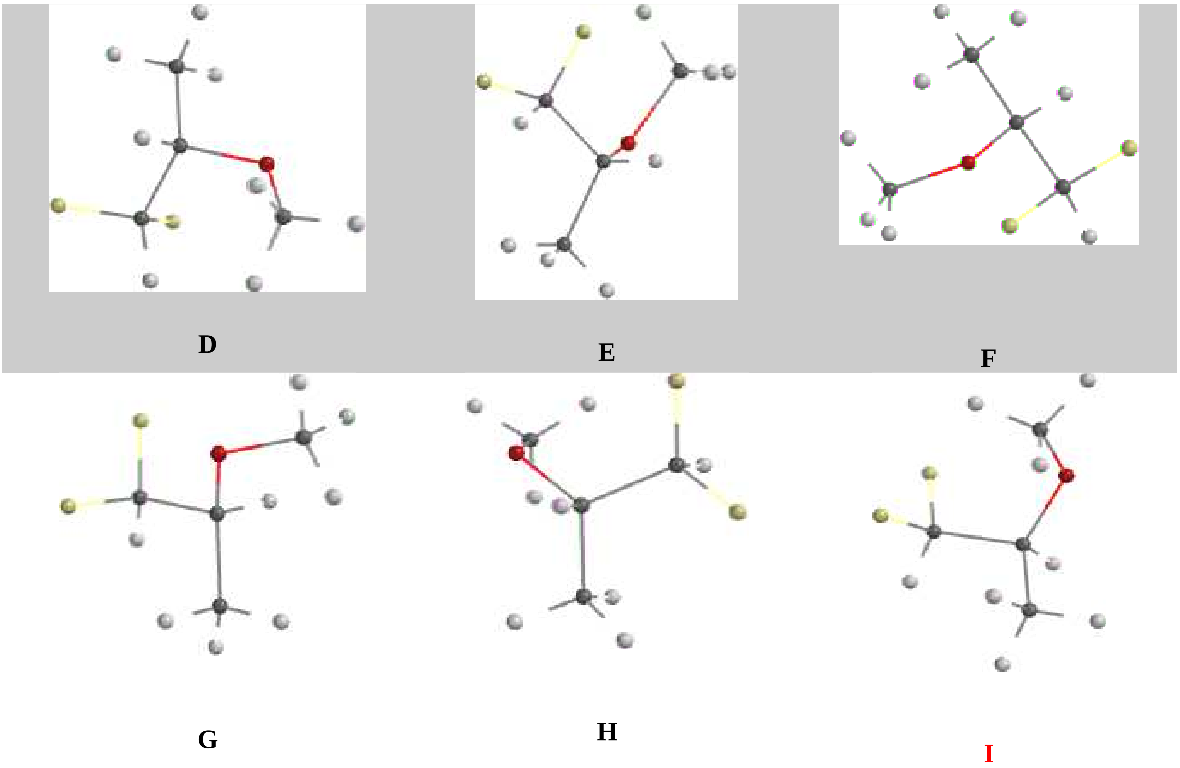

Fig. 1- 3D structures of the possible conformers of 1,1-difluoro-2-methoxypropane molecule

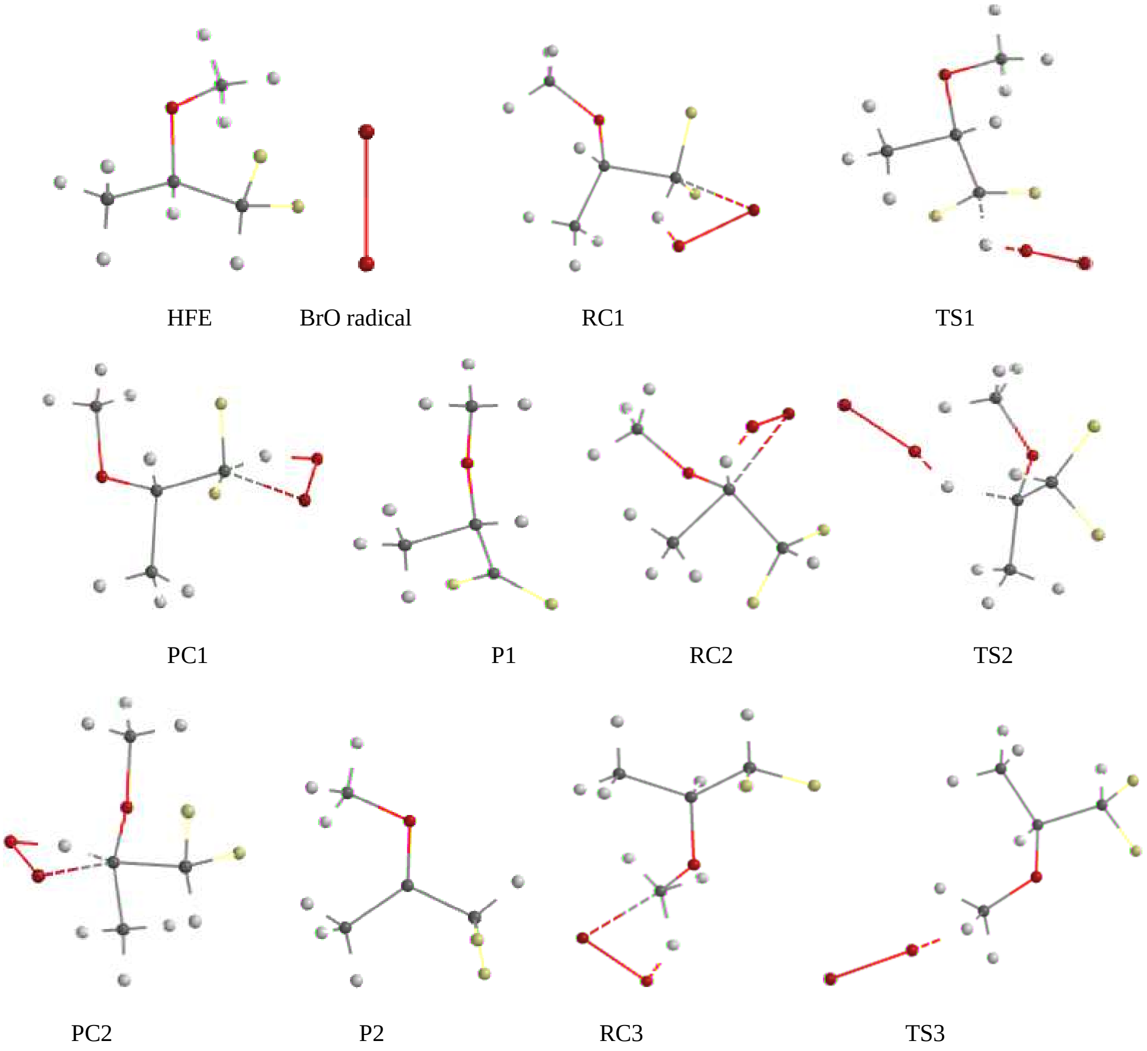

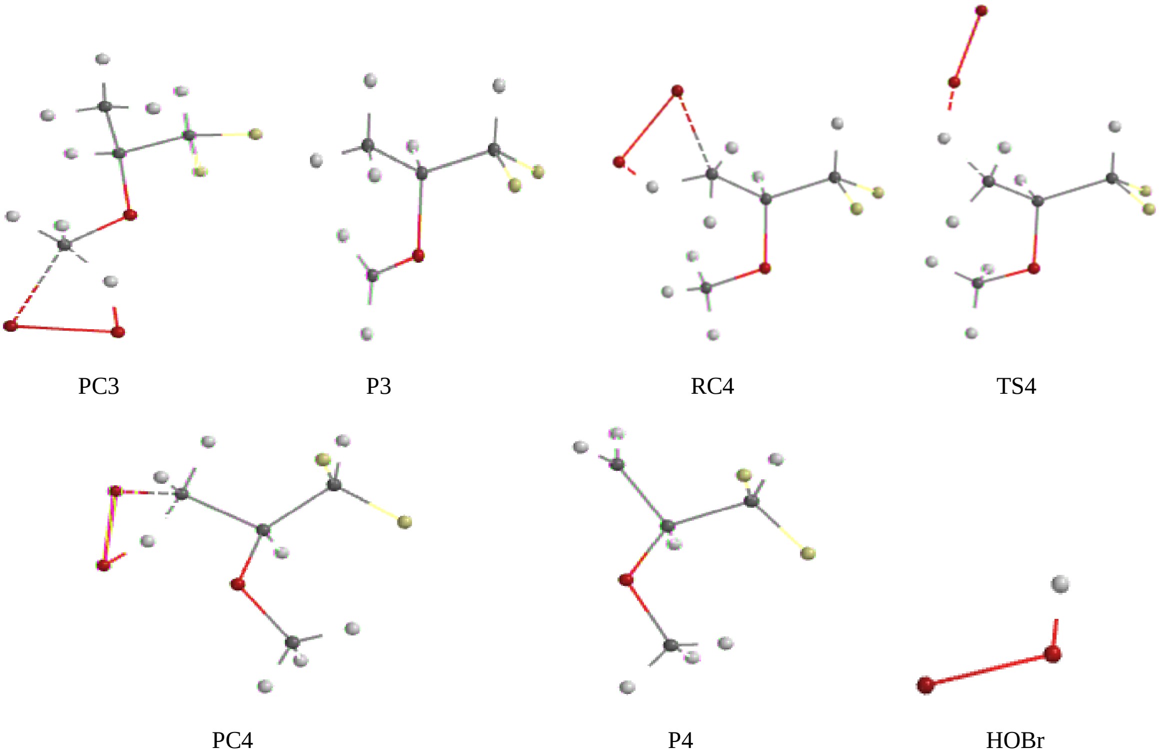

PC3 P3 RC4 TS4

PC4 P4 HOBr

Figure 2- 3D structures of optimized reacting species with BrO radical.

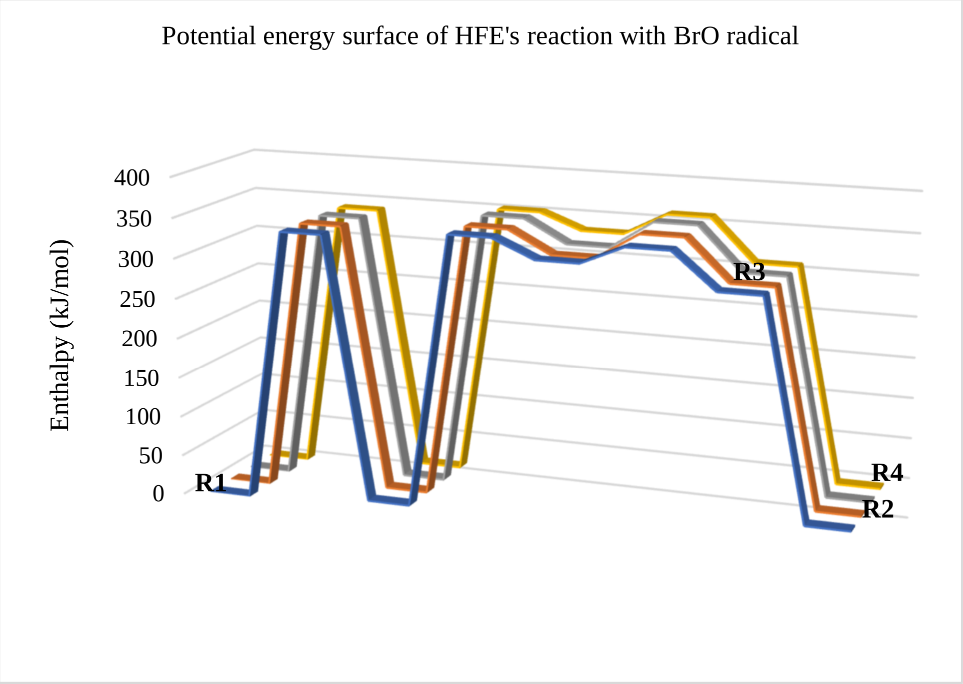

Figure 3- HFE vs BrO radical H-abstraction reaction channels (DFT/M06-2X/6-311++G(2df,2p)).

5. TABLES

Table 1 - Calculated energy (kJ mol^{-1}) of the optimized reacting species with BrO radical (298 K) at DFT/M06-2X/6-311++G** level of theory.

Reaction routes	HFE (kJ mol^{-1})	Radical (kJ mol^{-1})	RC (kJ mol^{-1})	TS (kJ mol^{-1})	PC (kJ mol^{-1})	P_{Major} (kJ mol^{-1})	P_{Minor} (kJ mol^{-1})
R1	-1134.32	-6955.47	-8089.87	-8089.32	-8089.89	-1131.86	-6956.99
R2	-1134.32	-6955.47	-8089.85	-8089.42	-8090.22	-1131.95	-6956.99
R3	-1134.32	-6955.47	-8089.66	-8089.52	-8090.32	-1131.89	-6956.99
R4	-1134.32	-6955.47	-8089.89	-8089.62	-8090.28	-1131.94	-6956.99

Table 2 - Improved Calculated energy (kJ mol^{-1}) of the optimized reacting species with BrO radical (298 K) at DFT/M06-2X/6-311++G(2df,2p) level of theory.

Reaction routes	HFE (kJ mol^{-1})	Radical (kJ mol^{-1})	RC (kJ mol^{-1})	TS (kJ mol^{-1})	PC (kJ mol^{-1})	P_{Major} (kJ mol^{-1})	P_{Minor} (kJ mol^{-1})
R1	-1134.39	-6955.56	-8089.85	-8089.30	-8089.78	-1131.94	-6957.08
R2	-1134.39	-6955.56	-8089.84	-8089.40	-8090.21	-1132.02	-6957.08
R3	-1134.39	-6955.56	-8089.86	-8089.49	-8090.35	-1131.96	-6957.08
R4	-1134.39	-6955.56	-8089.88	-8089.59	-8090.30	-1132.02	-6957.08

P_{Major}: Major product = hydrofluoroether radical & P_{Minor}: Minor product = HOBr

Table 3 - Calculated enthalpy (kJ mol^{-1}) of the optimized reacting species with BrO radical (298 K) at DFT/M06-2X/6-311++G** level of theory.

Reaction routes	HFE (kJ mol^{-1})	Radical (kJ mol^{-1})	RC (kJ mol^{-1})	TS (kJ mol^{-1})	PC (kJ mol^{-1})	P_{Major} (kJ mol^{-1})	P_{Minor} (kJ mol^{-1})
R1	338.40	12.54	349.61	327.38	352.09	307.06	44.25
R2	338.40	12.54	349.28	322.22	356.49	304.84	44.25
R3	338.40	12.54	351.70	323.40	361.40	306.76	44.25
R4	338.40	12.54	349.64	330.17	361.75	307.26	44.25

Table 4 - Improved Calculated enthalpy (kJ mol^{-1}) of the optimized reacting species with BrO radical (298 K) at DFT/M06-2X/6-311++G(2df,2p) level of theory.

Reaction routes	HFE (kJ mol^{-1})	Radical (kJ mol^{-1})	RC (kJ mol^{-1})	TS (kJ mol^{-1})	PC (kJ mol^{-1})	P_{Major} (kJ mol^{-1})	P_{Minor} (kJ mol^{-1})
R1	339.15	12.86	350.88	328.39	351.26	307.98	44.63
R2	339.15	12.86	350.45	323.45	355.90	305.97	44.63
R3	339.15	12.86	353.56	325.78	359.89	307.16	44.63
R4	339.15	12.86	351.34	331.80	359.28	307.49	44.63

Table 5 - Thermodynamics data on H-abstraction reaction channels (R1–R4) of the HFE with BrO radical calculated at DFT/M06-2X/6-311++G** Density Functional Theory.

Reaction routes	$\Delta_r H^o{}_{rxn}$ (kJ mol^{-1})	$\Delta_r G^o{}_{rxn}$ (kJ mol^{-1})	$\Delta_r E^o{}_{rxn}$ (kJ mol^{-1})	$\Delta G^{\dagger}$
R1	-0.37	-4.93	940.75	205.31
R2	-1.85	-7.81	857.21	200.49
R3	0.07	-4.41	907.77	198.11
R4	0.57	-4.27	860.86	209.65

Table 6 - Thermodynamics data on H-abstraction reaction channels (R1–R4) of the HFE with BrO radical calculated at DFT/M06-2X/6-311++G(2df,2p) Density Functional Theory.

Reaction routes	$\Delta_r H^o{}_{rxn}$ (kJ mol^{-1})	$\Delta_r G^o{}_{rxn}$ (kJ mol^{-1})	$\Delta_r E^o{}_{rxn}$ (kJ mol^{-1})	$\Delta G^\dagger$
R1	0.60	-4.22	928.21	205.62
R2	-1.41	-7.63	847.31	201.42
R3	-0.22	-5.00	901.84	201.08
R4	0.11	-5.10	843.65	212.11

Table 7 - DFT/M06-2X/6-311++G** thermodynamics parameters for the steps involved in the four HFEs reaction channels (R1-R4) with BrO radical

Reaction routes	$\Delta H^{\#}$(kJ mol^{-1})	$\Delta G^{\#}$(kJ mol^{-1})	ΔH_1(kJ mol^{-1})	ΔG_1(kJ mol^{-1})
R1	-23.56	-150.55	23.93	103.06
R2	-28.72	-158.38	26.87	102.79
R3	-27.54	-157.24	27.61	102.09
R4	-20.77	-145.56	21.34	103.18

Table 8 - DFT/M06-2X/6-311++G(2df,2p) thermodynamics parameters for the steps involved in the four HFEs reaction channels (R1-R4) with BrO radical

Reaction routes	$\Delta H^{\#}$(kJ mol^{-1})	$\Delta G^{\#}$(kJ mol^{-1})	ΔH_1(kJ mol^{-1})	ΔG_1(kJ mol^{-1})
R1	-23.62	-150.61	24.22	102.77
R2	-28.56	-158.22	29.16	100.50
R3	-26.23	-155.93	26.83	102.87
R4	-20.21	-145.00	20.81	103.98

$\Delta G^{\#}$= Gibb's free energy of transition state, ΔG_1= Gibb's free energy of product formation
$\Delta H^{\#}$= Enthalpy of transition state formation, ΔH_1= Enthalpy of product formation

Table 9 - IRC calculation results on transition states of each reaction channel for BrO radical at DFT/M06-2X/6-311++G**

Reaction routes	Transition states	Intrinsic reaction coordinate (IRC) in cm^{-1}
R1	TS1	i418
R2	TS2	i369
R3	TS3	i297
R4	TS4	i180

Table 10 - IRC calculation results on transition states of each reaction channel for BrO radical at DFT/M06-2X/6-311++G(2df,2p)

Reaction routes	Transition states	Intrinsic reaction coordinate (IRC) in cm^{-1}
R1	TS1	i520
R2	TS2	i450
R3	TS3	i397
R4	TS4	i280

Table 11 - BR, k and E_a of H-abstraction reaction of HFE with BrO radical at DFT/M06-2X/6-311++G(2df,2p)

Reaction routes	BR_{BrO}	k_{BrO} (cm^{-3} molecule^{-1} sec^{-1})	$E_{a_{BrO}}$ (kJ mol^{-1})
R1	94.50	4.10*10^{-06}	29.65
R2	2.53	1.10*10^{-07}	22.04
R3	1.80	7.80*10^{-08}	24.33
R4	1.18	5.10*10^{-08}	35.26

6. CONCLUSION

In this Insilco study, an oxidation reaction mechanism of 1,1-difluoro-2-methoxypropane with the BrO radical was investigated using two different levels of DFT (M06-2X/6-311++G** and M06-2X/6-311++G(2df,2p). This resulted to H-abstraction from the molecule which was more favored at $-\mathrm{OCH(CH_3)}$ carbon site. The whole reaction was found to proceeded in four plausible reaction channels (R1, R2, R3 and R4) with R2 being thermodynamically and kinetically most favorable channel. An intrinsic reaction coordinate (IRC) calculation carried out proved the transition states observed via each reaction channel as chemical species with all chemical properties to generate a pathway that can lead to the reactants and then to the products. The total rate constant of $4.34 * 10^{-06}$ cm^{-3} $molecule^{-1}$ sec^{-1} was reported for this study at DFT/M06-2X/6-311++G(2df,2p) level with an atmospheric lifetime (ALT) and GWP of 1.8 years and 165.30 respectively. Based on the results obtained, it was concluded that fluorinated HFE investigated can serves as a good substantial substitute for CFCs due to its short atmospheric lifetime and lower GWP.

ACKNOWLEDGEMENT

Mohammed Rufai Abubakar acknowledges the financial support of Petroleum Technology Development Fund (PTDF), Abuja, Nigeria, for providing a PTDF M.Sc. award (Award Letter No: PTDF/ED/LSS/MSc/MRA/244/17).

REFERENCES

ANDERSON, J.G. FREE RADICALS IN THE EARTH'S ATMOSPHERE: Their Measurement and Interpretation. **Ann. Rev. Phys. Chem.**, v. 38, p. 489 – 520, 1987.

BAIDYA, B.; LILY, M.; CHANDRA, A.K. Theoretical study on atmospheric chemistry of $CHF_2CF_2CH_2OH$: Reaction with OH radicals, lifetime and global warming potentials. **Computational and Theoretical Chem.**, v. 1119, p. 1 – 9, 2017.

CHRISTENSEN, L.K.; SEHESTED, J.; NIELSEN, O. J.; BILDE, M.; WALLINGTON, T. J.; GUSCHIN, A.; MOLINA, L. T.; MOLINA, M. J. Atmospheric Chemistry of HFE-7200 ($C_4F_9OC_2H_5$): Reaction with OH Radicals and Fate of $C_4F_9OCH_2CH_2O(\bullet)$ and $C_4F_9OCHO(\bullet)CH_3$ Radicals. **J. Phys. Chem. A.**, v. 102, n. 25, p. 4839-4845, Feb./April. 1998.

DEKA, R.C.; MISHRA, B.K. Theoretical studies on kinetics, mechanism and thermochemistry of gas – phase reactions of HFE – 449mec-f with OH radicals and Cl atom. **J Molecular Graphics and Modeling**, v. 53, p. 23-30, Jul. 2014.

DE CARVALHO, E. F. V.; ROBERTO-NETO, O. Effects of Multidimensional Tunneling in the Kinetics of Hydrogen Abstraction Reactions of O (^{3}P) with CH_3OCHO. **Journal of Computational Chemistry**, p. 1-9, Jan./Feb. 2018.

ESPINOSA-GARCIA, J. Ab Initio and Variational Transition – State Theory of the $CF_3CF_2OCH_3$ + OH Reaction Using Integrated Methods: Mechanism and Kinetics. **J. Phys. Chem. A.**, v. 107, n. 10, p. 1618- 1626, Jul./Dec. 2003.

GALANO, A.; ALVAREZ-IDABOY, J.R.; FRANCISCO-MARQUEZ, M. Mechanism and Branching Ratio of Hydroxyl Ethers + OH Gas Phase Reactions: Relevance of H Bond Interactions. **J. Phys. Chem. A.**, v. 144, n. 28, p. 7525-7536, April/May. 2010.

GARFIELD, E. Ozone-Layer Depletion: Its Consequences, the Causal Debate, and International Cooperation. **Essays of an Information Scientist: Science Literacy, Policy, Evaluation and other Essays**, v. 11, p. 39-49, 1988.

GOOD, D.A.; FRANCISCO, J.S.; JAIN, A.K.; WUEBBLES, D.J. Lifetime and global warming potentials for Dimethyl ether and for fluorinated ethers: CH_3OCH_3 (E143a), CHF_2OCHF_2 (E134), CHF_2OCF_3 (E125). **Journal of Geophysical Research**, v. 103, n. D21, p. 28186-28186, Nov. 1998.

GOUR, N.K.; MISHRA, B.K.; HUSSAINI, I.; DEKA, R.C. Theoretical Investigation on the kinetics and Thermochemistry of H-atom abstraction reactions of 2-chloroethyl methyl ether ($CH_3OCH_2CH_2Cl$) with OH radical at 298 K. **struct. Chem.**, p. 1 – 9, march/May. 2016.

GUO, Q.; ZHANG, N.; UCHIMARU, T.; CHEN, L.; QUAN, H.; MIZUKADO, J. Atmospheric chemistry of cyc-$CF_2CF_2CF_2CH{=}CH$–: Kinetics, products, and mechanism of gas-phase reaction with OH radicals, and atmospheric implications. **Atmospheric Environment**, v. 179, p. 69-76, Jan./Feb. 2018.

HASHEMI, S.R.; SAHEB, V. Theoretical Studies on the Mechanism and Kinetics of the Hydrogen Abstraction Reactions of threo- $CF_3CHFCHFC_2F_5$ and erthro- $CF_3CHFCHFC_2F_5$ (HFC-43-10mee) by OH radicals. **Computational & Theoretical Chemistry**, p. 1-28, May/Sept. 2017.

HURLEY, M. D.; WALLINGTON, T. J.; ANDERSEN, M. P. S.; ELLIS, D. A.; MARTIN, J. W.; MABURY, S. A. Atmospheric Chemistry of Fluorinated Alcohols: Reaction with Cl Atoms and OH Radicals and Atmospheric Lifetimes**. J. Phys. Chem. A**, v. 108, n. 11, p. 1973-1979, Oct./Jan. 2004.

LASZLO, B.; ROBERT, E.H.; MICHAEL, J.K.; ANDRZEJ, W.M. Kinetic studies of the reactions of BrO and IO radicals. **Journal of Geophysical Research**, v. 102, n. D1, p. 1523-1532, Jan. 1997.

MABURY, S. A.; YOUNG, C. J.; HURLEY, M. D.; WALLINGTON, T. J. Atmospheric Lifetime and Global Warming Potential of a Perfluoropolyether. **Environ. Sci. Technol**., v. 40, n. 7, p. 2242-2246, Oct./Jan. 2006.

MOLINA, J.M.; ROWLAND, F.S. Stratospheric sink for chlorofluoromethanes: chlorine atom-catalyzed destruction of ozone. **Nature**, v. 249, p. 810-812, Jun. 1974.

ORKIN, V. L.; VILLENAVE, E.; HUIE, R. E.; KURYLO, M. J. Atmospheric Lifetimes and Global Warming Potentials of Hydrofluoroethers: Reactivity toward OH, UV Spectra, and IR Absorption Cross Sections. **J. Phys. Chem. A**, v. 103, n. 48, p. 9770-9779, May/Sept. 1999.

PAPADIMITRIOU, V.C.; PAPANASTASIOU, D.K.; STEFANOPOULOS, V.G.; ZARAS, A.M.; LAZAROU, Y.G.; PAPAGIANNAKOPOULOS, P. Kinetics study of the Reactions of Cl Atoms with

$CF_3CH_2CH_2OH$, $CF_3CF_2CH_2OH$, $CHF_2CF_2CH_2OH$ and $CF_3CHFCF_2CH_2OH$. **J. Phys. Chem. A.**, v. 111, n. 45, p. 11608 – 11617. Jun./Aug. 2007.

PHILIP, M. Advanced chemistry. Cambridge Low Price Edition, UK: 1996.

PRATHER, M.; SPIVAKOVSKY, C.M. Tropospheric OH and the Lifetimes of Hydrochlorofluorocarbons. **Journal of Geophysical Research**, v. 95, n. D11, 18723-18729, Oct. 1990.

ROHRER, F.; BERRESHEIM, H. Strong correlation between levels of Tropospheric hydroxyl radical and solar ultraviolet radiation. **Nature**, v. 442, p. 184-187, Jul. 2006.

ROUSSEL, M. R. Transition State Theory (Chemistry and Biochemistry), 3rd ed. University of Lethbridge, Canada: 2009.

ROWLAND, F.S. Stratospheric Ozone depletion. **Phil. Trans. R. Soc. B**, v. 361, p. 769-790. 1996.

ROWLEY, D. M.; FERRACCI, V. Kinetic studies of the BrO + ClO cross-reaction over the range T = 246–314 K. **Phys. Chem.**, v. 16, p. 1182-1196, Aug./Oct. 2014.

SAKO, T.; SATO, M.; NAKAZAWA, N.; OOWA, M.; YASUMOTO, M.; ITO, H.; YAMASHITA, S. Critical Properties of Fluorinated Ethers. **J. Chem. Eng. Data**, v. 41, n. 4, p. 802-805, Dec./May. 1996.

SCHLAGER, H.; GREWE, V.; ROIGER, A. Chemical composition of the atmosphere. **Springer**, p. 17-35, 2012.

SIAKA, A.A.; UZAIRU, A.; IDRIS, A.; ABBA, H. Thermodynamics and Kinetics of Spiro – Heterocycle Formation Mechanism: Computational Study. **Phys. Chem. Res**., v. 5, n. 3, p. 439-446, Jan./Feb. 2017.

SPARTAN '14 v 114. Wave function, Inc., Irvine. 2013.

TRUHLAR, D. G.; GARRETT, B. C.; KLIPPENSTEIN, S. J. Current Status of Transition-State Theory. **J. Phys. Chem.,** v. 100, n. 31, p.12771-12800, Dec./Feb. 1996.

WANG, Y-N.; CHEN, J.; LI, X.; WANG, B.; CAI, X.; HUANG, L. Predicting rate constants of hydroxyl radical reactions with organic pollutants: Algorithm, Validation, applicability domain and mechanistic interpretation. **Atmospheric Environment**, v. 43, p. 1131-1135, Oct./Nov. 2009.

WHITE, C.W.; MARTELL, J.M. Hydrogen Abstraction from Fluorinated Ethyl Methyl Ether System by OH Radicals. **Advances in Physical Chemistry**, v. 2016, n. 3740278, p. 1-10, Jul./Nov. 2015.

WOFSY, S. C.; MCELROY, M. B.; YUNG, Y. L. The chemistry of atmospheric Bromine. **Geophysical Research Letters**, v. 2, n. 6, p. 215-218, Jun. 1975.

WORLD METEOROLOGICAL ORGANIZATION PROJECT – Report No. 52 Scientific Assessment of Ozone Depletion: Geneva Switzerland, ISBN: 9966-7319-6-2. 2010.

YANG, L.; LIU, J-Y.; WANG, L.; HE, H-Q.; WANG, Y.; LI, Z-S. Theoretical Study of the Reactions $CF_3CH_2OCHF_2$ + OH/Cl and its Product Radicals and Parent Ether ($CH_3CH_2OCH_3$) with OH. **J Comput. Chem.**, v. 29, n. 4, p. 550–561, Jan./Jul. 2007.

YE, J-T.; BAI, F-Y.; PAN, X-M. Computational Study of H-abstraction reactions from $CH_3OCH_2CH_2Cl/CH_3CH_2OCH_2CH_2Cl$ by Cl atom and OH radical and fate of alkoxy radicals. **Environ. Sci. Pollut. Res.**, v. 23, p. 23467–23484, may/Aug. 2016.